INORGANIC CHEMISTRY FRONTIERS

RESEARCH ARTICLE

View Article Online
View Journal

Cite this: DOI: 10.1039/d6qi00270f

Easily available *click* ligands enable iridium-catalysed aromatic C–H borylation with proximal selectivity: the critical role of solvent and B_2pin_2 in catalyst modification under *operando* conditions

Vanessa Delahaye, Thierry Roisnel, Sylvie Dérien, * Mathieu Achard * and Rafael Gramage-Doria *

Transition metal-catalyzed C–H functionalization provides a powerful platform for the efficient synthesis of complex molecules, with iridium-catalyzed C–H borylation representing a cornerstone of this field. Fine-tuning *N*,*N*-chelating ligands effectively controls remote selectivity in aromatic substrates, whereas achieving proximal (*ortho*) selectivity typically requires preformed iridium complexes or highly sophisticated, air-sensitive ligands. Herein, we report a convenient and modular synthesis of sustainable ligands *via* cost-effective copper-catalyzed *click* chemistry. Although the resulting pyridyl–triazolyl ligands are in principle designed for neutral *N*,*N*-chelation, they preferentially adopt an anionic *N*,*C*-chelating mode under catalytically relevant conditions. This behavior arises from triazolyl proton abstraction promoted by excess bis(pinacolato)diboron (B_2pin_2) and the use of polar, coordinating solvents. Control experiments, spectroscopic analysis, and kinetic studies support this mechanistic scenario. As a consequence, sterically demanding substrates, including phthalimides and related carbonyl-containing aromatics, undergo efficient proximal C–H borylation. Overall, this work underscores the importance of catalyst structural evolution under reaction conditions and highlights a general design principle that may apply to other transition metal-catalyzed atom-economical processes.

Received 5th February 2026,
Accepted 16th April 2026

DOI: 10.1039/d6qi00270f

rsc.li/frontiers-inorganic

Introduction

Transition metal-catalysed C–H functionalization has expanded rapidly, enabling efficient access to complex molecules from minimally functionalized substrates.[1–6] As a result, atom- and step-economical strategies continue to enrich the synthetic toolbox.[7–12] Further expansion of chemical space requires a detailed understanding of catalyst behaviour to anticipate and control reactivity, particularly to modify established selectivity patterns and to improve catalyst activity and stability.

In this context, iridium-catalysed C–H borylations have been widely studied and applied in the pharmaceutical industry and academia since the pioneering discoveries from Ishiyama, Hartwig and Miyaura.[13–17] They demonstrated the suitability of *N*,*N*-chelating ligands to form catalytically active iridium-tris-boryl species to achieve C–H borylations at the most sterically accessible site of the molecule of interest, similarly to *P*,*P*-chelating ligands.[18] The last few decades have witnessed the boost of the field with the rational design of different classes of ligands in order to achieve highly efficient regio-, enantio- or stereo-controlled iridium-catalysed C–H borylations[19–22] due to the versatile post-functionalization of boron-containing groups.[23–25]

In the case of aromatic C–H borylations, remote attractive interactions between substrates and catalysts have been mastered for controlling the *meta*/*para* selectivity with modified versions of bipyridine ligands being of choice.[26–36] On the other hand, achieving *ortho* selectivity in iridium-catalysed aromatic C–H borylations is not trivial because it is sterically less accessible and requires, initially, the use of monodentate ligands derived from arsenic or fluorinated phosphines as shown by Miyaura (Fig. 1, top).[36,37] Further research led to the use of highly sophisticated and air-sensitive *P*-, *Si*- and *B*-containing heteroditopic ligands **L1–L4** developed, independently, by Maleczka & Smith,[38–40] Li,[41] and Xu[42–46] (Fig. 1, top), which are accessible *via* energetically demanding cryogenic chemistry (*i.e.* organolithium reagents) and are postulated to behave as anionic ligands upon coordination to iridium (**Ir-1**, Fig. 1, top). Equally efficient is the strategy relying on the beforehand preparation of well-defined iridium complexes such as **Ir-PTY**, which consists of a *S*-containing

Univ Rennes, CNRS, ISCR – UMR6226, F-35000 Rennes, France.
E-mail: sylvie.derien@univ-rennes.fr, mathieu.achard@univ-rennes.fr, rafael.gramage-doria@univ-rennes.fr

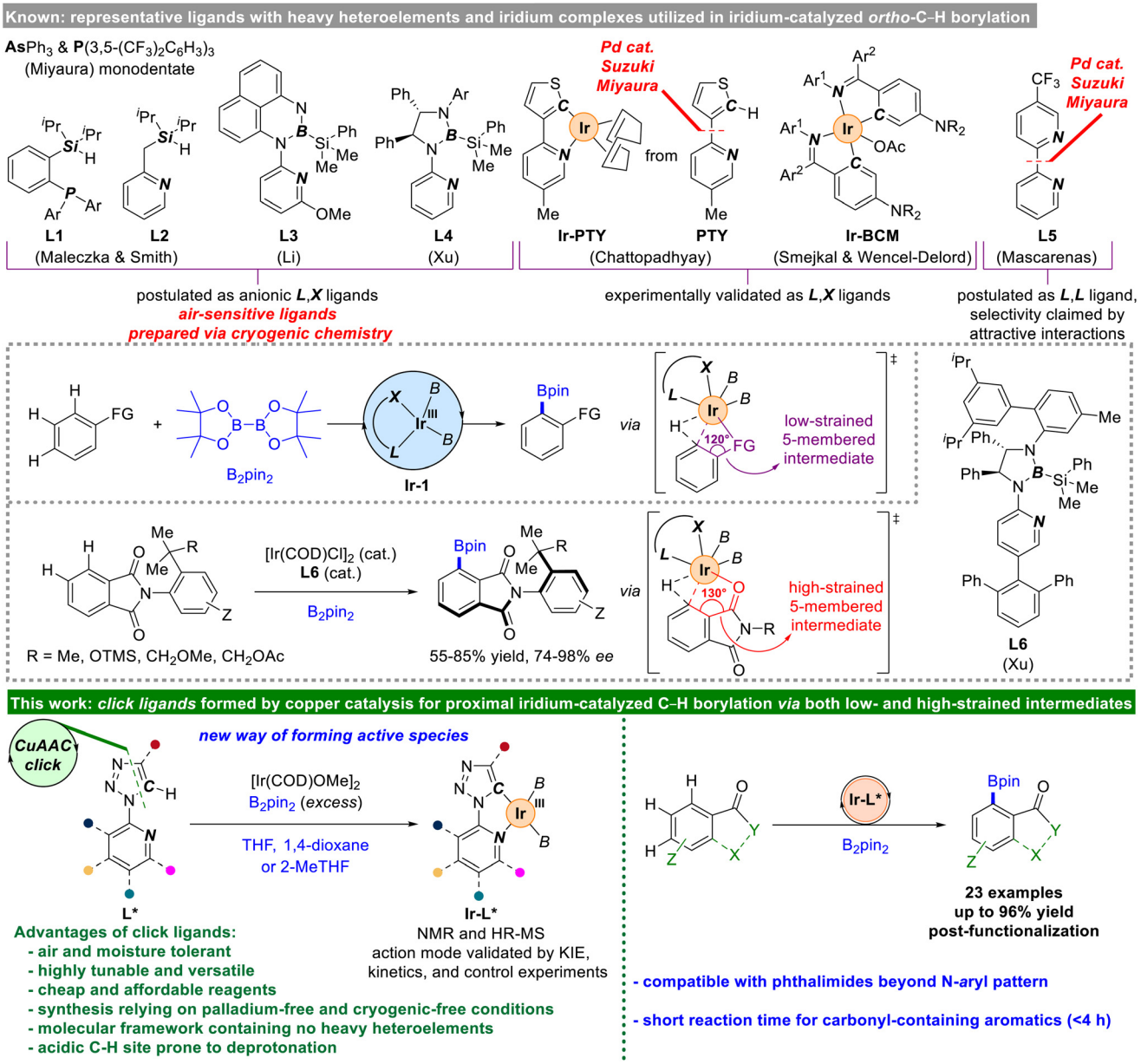

Fig. 1 State-of-the-art of the iridium-catalysed *ortho*-C–H bond borylation in aromatics (top) and the current strategy based on *click* ligands including mechanistic considerations and applicability (bottom). FG = functional group amenable to transient coordination with the iridium centre, Ar = aryl, *B* = (boron)pinacolato, Ar^1 = *p*-^{t}Bu-C_6H_4, Ar^2 = *p*-NR_2-C_6H_4 (R = Et and Pr), COD = 1,5-cyclooctadiene, X = CO or H, and Y = NR_2, R, or OR.

N,*C*-chelating ligand (**PTY**) that is prepared *via* costly palladium-catalysed cross-coupling chemistry by Chattopadhyay's group[47] or the bis-cyclometallated iridium catalysts **Ir-BCM** developed by Wencel-Delord and Smejkal (Fig. 1, top).[48,49] Alternatively, and beyond Sawamura's heterogeneous system,[50] Mascarenas (**L5**, Fig. 1, top),[51] Reek,[52] and others,[53,54] independently, reported iridium-catalysed *ortho*-C–H borylation with attractive remote interactions between the substrate and the catalyst claimed to explain the selectivity.

It appears obvious that a major issue for the broad implementation of iridium-catalysed C–H borylations is the affordability of ligands that form highly powerful iridium catalysts. Consequently, aiming at diversifying the structural nature of the ligand frameworks while simultaneously broadening the accessibility for ligands enabling challenging *ortho*-selective C–H borylations under iridium catalysis, we anticipated that *click* ligands **L*** (Fig. 1, bottom) formed *via* copper-catalysed azide–alkyne cycloadditions (**CuAAC**), also known as *click* chemistry, may represent a unique entry.[55–57] These *click* ligands are straightforward to access using catalysts based on more abundant and affordable copper while increasing molecular diversity and upgrading chemical stability.[58–61] In addition, based on the fact that the triazolyl core features a relatively acidic C–H bond[62,63] comparable to that found in

thiophenes[64,65] such as in ligand **PTY**,[47] we anticipated that *in situ* proton abstraction may lead to anionic *L*,*X*-type ligands prone to chelate iridium.[66,67] In this respect, we herein demonstrate, for the very first time, that bis(pinacolato)diboron (B_2pin_2) behaves as both a borylating agent and mediator in proton abstraction at the *click* ligand in the presence of iridium, thereby forming the active iridium(III)-bis-boryl species **Ir-L*** (Fig. 1, bottom) under *operando* conditions according to in-depth mechanistic investigations. Such a unique event, which takes place under conditions relevant to catalysis, is further strongly facilitated by the nature of the solvent, being polar coordinating ones such as THF, 1,4-dioxane or bio-sourced 2-MeTHF of choice.

Moreover, we herein tackle the proximal C–H borylation of phthalimides,[68] useful difunctionalized aromatics that are key intermediates for the further elaboration of biologically-relevant scaffolds as well as promising dyes, porous solids, and polymers.[69–72] Such a class of substrates, which are based on a benzene core 1,2-doubly fused with a small five-membered imide ring, are extremely challenging to activate at the proximal C–H site because the postulated key C–H-activated iridacycle intermediate will have to overcome a highly strained 130° angle between the carbonyl directing group, the iridium centre and the proximal C–H site (Fig. 1, top). In this respect, Xu and co-workers reported the sole example of proximal, enantioselective C–H borylation of prochiral *N*-arylphthalimides comprising bulky substituents in the *ortho* position of the aryl units using the highly elaborated ligand **L6** (Fig. 1, top).[73] In a complementary manner, the herein reported *click* ligands compare well in terms of activity and selectivity for phthalimides beyond *N*-aryl-substituted patterns (Fig. 1, bottom). The applicability of the herein developed *click* ligands in iridium-catalysed proximal C–H borylation is further demonstrated to other synthetically useful carbonyl-containing aromatic substrates operating under relatively short reaction times compared to current state-of-the-art catalytic systems (Fig. 1, bottom). This work gives a glimpse that structural ligand modification during catalysis, promoted by both reagents and solvents, is beneficial and does not lead to undesired catalyst deactivation pathways, thereby underlining the importance and challenge of identifying the truly active species under *operando* conditions in metal-catalysed C–H bond functionalization.[74,75]

Results and discussion

Preparation of a library of *click* ligands and activation mode at iridium

In order to develop a library of *click* ligands with different steric and electronic properties around a sigma donor 2-pyridyl motif, ligands **A–F** were accessed by reacting the corresponding alkynes (phenylacetylene or 2-pyridylacetylene) with 2-azido-pyridyl derivatives using copper catalysts, namely $Cu(PPh_3)_3Br$ and $Cu(OTf)_2$ (Scheme 1, left).[76–78] This methodology also made possible to obtain ligand **G** in which the triazolyl core is flanked by two phenyl groups. An alternative two-step strategy was more convenient to prepare ligands **H–N** (Scheme 1, right), which is based on the formation of key 1-tosyl-1*H*-1,2,3-triazolyl derivatives under copper catalysis followed by a nucleophilic addition to bench stable pyridine-*N*-oxide reagents.[79–83] As such, a convenient library of 14 *click* ligands was straightforward prepared by means of a cheap and sustainable key copper-catalysed azide–alkyne cycloaddition (**CuAAC**).

Furthermore, we obtained single crystals suitable for X-ray diffraction (SCXRD) studies for two of these ligands (**A** and **K**, Scheme 1), which revealed an almost perfect co-planarity between the (hetero)aromatic rings and the triazolyl core with relatively small dihedral angles of 4.5° and 13.2° in **A** and 11.5° and 14.6° in **K**. In addition, the nitrogen atom from the 2-pyridyl ring faces the hydrogen atom from the triazolyl core with N···H–C short distances of 2.66 Å for *click* ligand **A** and 2.71 Å for *click* ligand **K** (Scheme 1). Solution NMR studies performed by means of ^1H–^1H NOESY experiments with ligand **K** in THF-d_8 solvent revealed a strong correlation between the hydrogen atom from the triazolyl C–H bond and the *ortho*-hydrogen atoms of the phenyl fragment (Scheme 1, right), thereby strongly supporting that the thermodynamically stable conformation observed in the solid state persists in solution as well.[84] This observation is likely the consequence of a destabi-

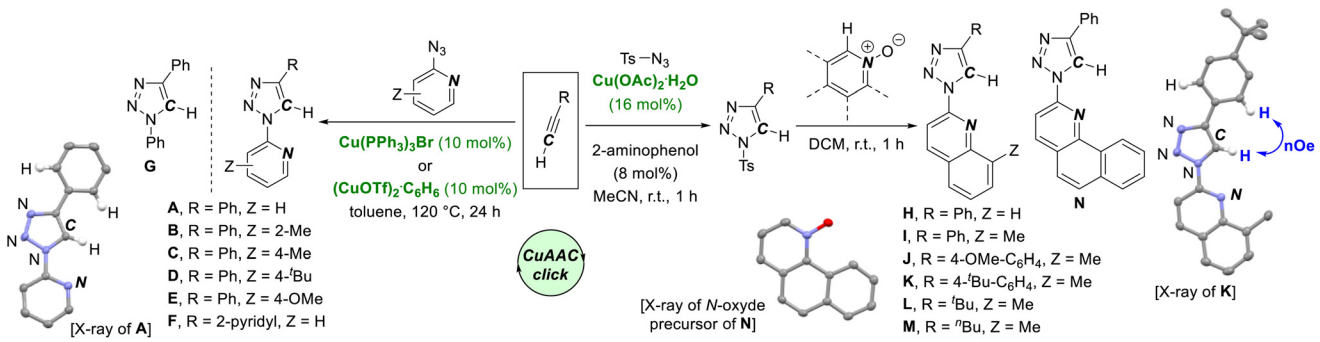

Scheme 1 Stepwise build-up of a library of *click* ligands (**A–N**) under **CuAAC** catalysis (for details, see the SI) including SCXRD of **A** (CCDC 2480983, left) and **K** (CCDC 2480984, right) and the *N*-oxide precursor of **N** (CCDC 2480985, middle – ORTEP drawings with thermal ellipsoids at 50% probability; selected hydrogen atoms are omitted for the sake of clarity). Ts = *p*-toluene sulfonyl.

lization effect for the opposite scenario in which the pyridyl ring rotates and its nitrogen lone pair faces the lone pair from the central nitrogen atom of the triazolyl core. It is worthy to note that the nitrogen lone pair from the pyridyl ring and the carbon lone pair that could result from the C–H abstraction at the triazolyl core are well pre-organized within these *click* ligands to undergo potential *L*,*X*-chelation towards an iridium metal centre.

Next, we evaluated the coordinating ability of the *click* ligands to iridium under *operando* conditions, namely conditions relevant for C–H bond borylation. For that, *click* ligand **A** was reacted with $[Ir(COD)OMe]_2$ (COD = 1,5-cyclooctadiene), which is the archetypical pre-catalyst employed in iridium-catalyzed C–H borylations, using undistilled THF-d_8 as the solvent (Fig. 2). In contrast to Chattopadhyay's ligand **PTY** that does readily undergo iridacycle formation at room temperature in THF solvent in the absence of B_2pin_2 (**Ir-PTY**, Fig. 1, top),[47] no reactivity was observed with *click* ligand **A** (Fig. 2, top), thereby indicating the less acidic character of the triazolyl C–H bond in **A** with respect to the α-thiophenyl C–H bond in **PTY**. On the other hand, upon addition of 10 equivalents of B_2pin_2 and heating at 65 °C, which are conditions that are employed in iridium-catalyzed C–H borylations, the proton signal from the C–H triazolyl core at δ = 9.5 ppm vanished (Fig. 2, bottom) with concomitant formation of signals ascribed to the iridium-coordinated COD ligand (δ = 5.6 ppm) and the borylated side-products, namely (HO)Bpin (δ_H = 6.7 ppm and δ_B = 22.4 ppm) and $O(Bpin)_2$ (δ_B = 21.3 ppm), according to ^1H and $^{11}B\{^1H\}$ NMR spectroscopy studies (Fig. S1–S7 in the SI), resulting from HBpin degradation due to the presence of water traces in the solvent.

In addition, HR-MS studies on this mixture revealed the formation of **Ir-A** species (m/z = 777.3329) involving the presence of two Bpin units and a deprotonated, anionic *click* ligand **A** engaged in *N*,*C*-chelation to iridium also bound to a COD ligand (Fig. S2 in the SI). The presence of $[(OH)(MeO)(Bpin)_2]$ species was also evidenced by HR-MS studies (Fig. S2 in the SI). We noted that *click* ligand **A** did not react with B_2pin_2 (10 equiv.) unless $[Ir(COD)OMe]_2$ was later added to the reaction mixture (Fig. S1 in the SI). These findings strikingly contrasts to the fact that *click* ligand **A** does readily undergo *N*,*N*-chelation at iridium in toluene solvent as reported by us previously.[34,35,54] As such, the nature the solvent, here THF, strongly influences the coordination of *click* ligand **A** to iridium under *operando* conditions.

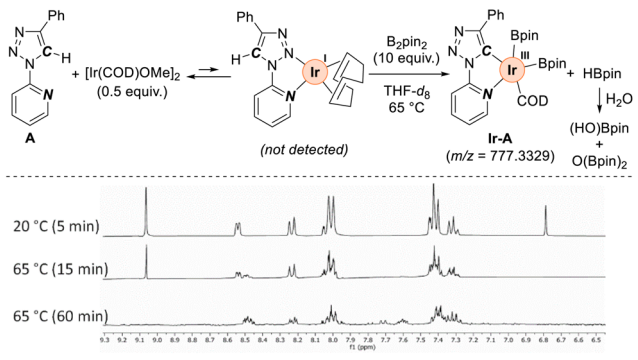

Fig. 2 Formation of **Ir-A** species under *operando* conditions inferred by ^1H NMR spectroscopy and HR-MS studies.

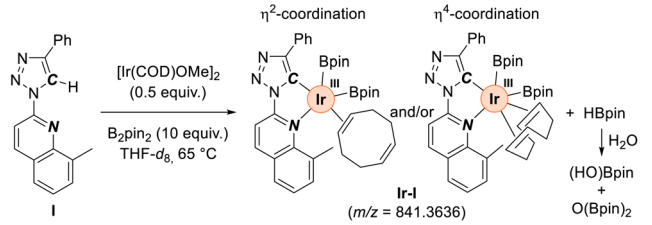

Scheme 2 Formation of **Ir-I** species under *operando* conditions inferred by ^1H NMR spectroscopy and HR-MS studies.

In order to study whether this behaviour is general to other *click* ligands, HR-MS studies were performed by combining *click* ligand **I**, the iridium precursor $[Ir(COD)OMe]_2$ and B_2pin_2 in THF-d_8 solvent at 65 °C (Scheme 2). Besides some signals resulting from mono-, bis- and tris-borylation of the *click* ligand, two major signals belonging to iridium species were identified (Fig. S8 in the SI). The first one, namely **Ir-I**, at m/z = 841.3636 corresponded to $[(\mathbf{I})Ir(Bpin)_2(COD)]$ (m/z = 841.3649) that could exist as a 16 and/or 18 electron complex depending on whether the COD ligand is engaged in η^2- or η^4-coordination to iridium (Scheme 2). The second iridium species at m/z = 966.4527 was consistent with **Ir-I** species being borylated at the *click* ligand or at the COD ligand. In addition, ^1H NMR studies also supported the formation of COD-ligated species (δ = 4.9–5.6 ppm) although multiple species were present most likely due to formation of conformers and/or the variable hapticity of the COD ligand when coordinating to iridium (Fig. S3–S8 in the SI).

The role of *click* ligands in tuning the regio-selectivity of iridium-catalysed C–H borylation of carbonyl-containing aromatic substrates

With a library of *click* ligands with diverse steric and electronic features in hand, and after effectively disclosing their unique coordinating ability to iridium as *L*,*X*-ligands under *operando* conditions, we screened their potential in the iridium-catalysed proximal C–H borylation of phthalimides that feature completely different substitution patterns compared to Xu's contribution with ligand **L6** (Fig. 1, top and Table S5 in the SI).[73] We first focused on the iridium-catalysed C–H borylation of *N*-methylphthalimide (**1a**) as a benchmark model, which can lead to proximal or distal borylated products **2a** and **3a**, respectively (Scheme 3). It is relevant to note that proximally-borylated **2a** constitutes a key intermediate for the elaboration of biologically-relevant aristolactam alkaloids.[85]

The reaction conditions applied consisted of 4 mol% of the ligand, 2 mol% of the $[Ir(COD)OMe]_2$ precursor and two equivalents of B_2pin_2 in freshly distilled THF at reflux for 48 hours (Scheme 3). As expected, using 4,4-di-*tert*-butyl-2,2′-bipyridine (**dtbpy**) or phenanthroline (**phen**) as the ligands,

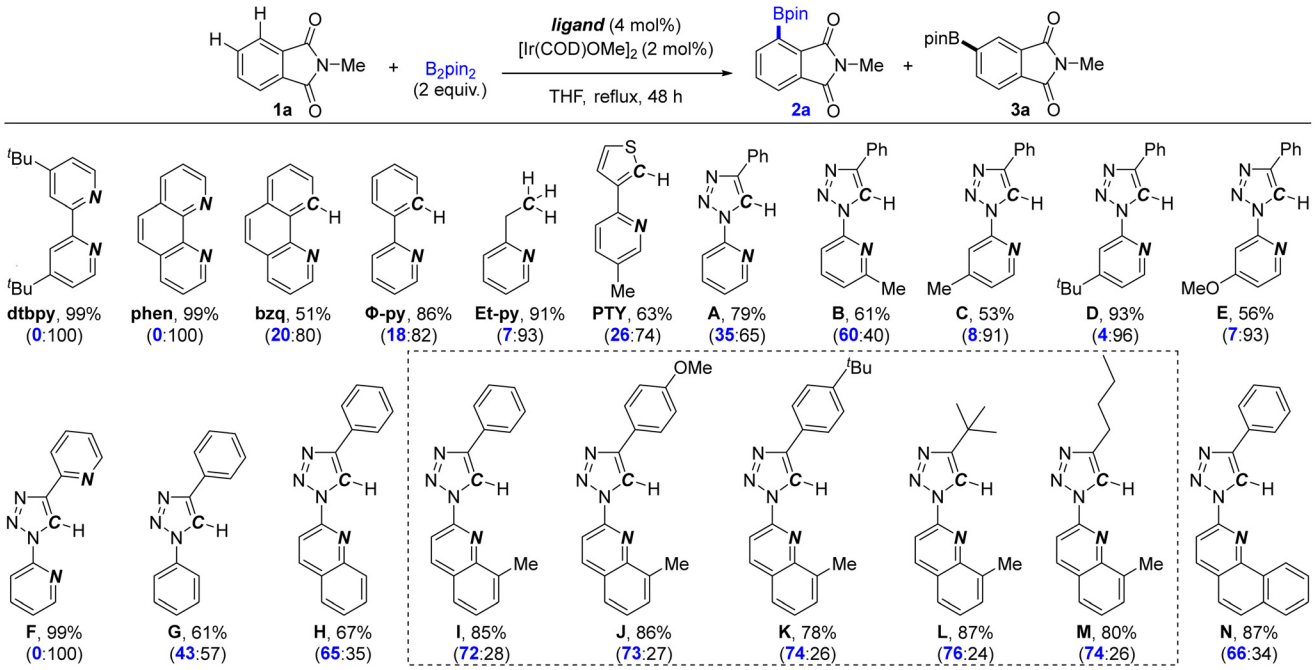

Scheme 3 Evaluation of ligands in the iridium-catalysed C–H borylation of *N*-methylphthalimide (conversion of **1a** in percentage and the ratio of **2a** : **3a** are displayed in brackets after being determined by GC analysis using dodecane as an internal standard).

independently, exclusively led to the distal C–H borylated product **3a** in quantitative yield in agreement with a highly favourable C–H activation event taking place at the most sterically accessible site in the substrate with a preference for the aromatic site over the *N*-methyl site, further corroborating the ease of reactivity under non-directed conditions.[86,87] Unexpectedly, using benzo[*h*]quinoline (**bzq**), which is structurally related to **phen** but with a nitrogen atom swapped by a CH group, increased the ratio of proximal borylated product **2a** to a promising 20% although with a low conversion of 51%. Similar results were observed with 2-phenylpyridine (**ϕ-py**) and to a less extent with 2-ethylpyridine (**Et-py**). For comparison purposes, Chattopadhyay's **PTY** ligand was utilized and it afforded 63% conversion and a percentage ratio of proximal *versus* distal of 26 : 74. Interestingly, using *click* ligands such as **A** gave rise to superior amounts of proximal borylated product **2a** up to 35% yield with a decent 79% conversion of **1a**. Remarkably, *click* ligand **B** that contains a 2-methyl substituent in the pyridyl ring completely reversed the regioselectivity, leading to proximal **2a** as the major product (60%), thus indicating that the substitution pattern in the pyridyl ring profoundly impacts the regioselectivity outcome in the iridium-catalysed C–H bond borylation. However, introducing different steric and electronic patterns in position 4 of the pyridyl ring (*click* ligands **C–E**) eroded the regioselectivity in favour of the distally-borylated product **3a** (91–96%). C*lick* ligand **F**, which contains two 2-pyridyl substituents around the triazolyl core afforded only the distally-borylated product **3a**. These findings suggest that *click* ligands **C–F** can also behave as *N*,*N*-chelators or mono-dentate ligands, leading to *L*,*L*-type iridium tris-boryl species (Scheme 11, top), which are more reactive than the *L*,*X*-type iridium species when exposed to a substrate such as **1a** that requires to reach a highly-demanding iridacycle intermediate with a 130° between the functional group, the iridium centre and the CH site for enabling proximal selectivity (Fig. 1, top).

Surprisingly, *click* ligand **G**, which contains no pyridyl unit, outperformed *click* ligand **A**, leading to 43% of proximal borylated product **2a** although with a modest conversion of **1a** (61%). C*lick* ligand **H**, in which the triazolyl core is linked to a quinoline unit, slightly outperformed *click* ligand **B** in terms of conversion (67%) and the formation of proximal borylated product **2a** (65%). Following this trend, *click* ligands **I–M** (Scheme 3, framed), which feature a bulky 8-methylquinoline unit linked to the triazolyl motif, revealed, gratifyingly, the highest conversions (up to 87%) with the proximal borylated product **2a** formed in up to 76% yield with minimal influence of the substitution pattern at the quaternary carbon atom from the triazolyl core. C*lick* ligand **N** that bears a 7,8-benzoquinoline motif did not surpass the activity or selectivity of *click* ligands **I–M**. Modification of reaction conditions (temperature, solvent, concentration, and variation of the stoichiometry of reagents) when using the most active and selective *click* ligands **I–M** (Scheme 3, framed) did not afford higher conversions nor improved proximal selectivity (Tables S1–S4 in the SI). We also noted that the reaction did not take place in the absence of the iridium precursor nor in the absence of the ligand. Other borylating reagents instead of B_2pin_2 such as HBpin, bis(neopentyl glycolato)diboron or bis(catecholato) diboron were tested but led to very low conversions not exceeding 30%.

The reactivity of diversely-functionalized phthalimide substrates was further evaluated using *click* ligand **I**, which gave a good balance of conversion/selectivity under iridium-catalysed C–H borylation conditions, leading to proximally-borylated products **2** while being only based on C, H, and N atoms (Scheme 4). The number of equivalents of B_2pin_2 was adjusted to 1.2 after slight fine-tuning of the reaction conditions in order to reduce undesired bis-borylated side-products (Tables S1–S4 in the SI). Due to the experimental difficulty of isolating some of the Bpin-containing products **2** derived from phthalimides, we also provided the isolated yields for the boronic acid post-functionalized products in Scheme 4.

The catalysis was tolerant to alkyl groups as shown in the reactivity of *N*-methylphthalimide that afforded the proximally borylated product **2a** in 70% selectivity and it was isolated as the corresponding boronic acid in 47% yield. Similar observations were encountered for the reactivity of *N*-(*p*-tolyl)phthalimide **1b**, in which no C–H borylation took place in the *p*-tolyl unit. 1-Naphthylphthalimide **1c** was borylated in the proximal position in an excellent 92% selectivity and 67% isolated yield with no detectable C–H borylation at the naphthalene core besides the presence of seven additional aromatic C–H bonds. Phthalimides containing synthetically useful handles such as ester and ether groups were tolerated and reacted with conversions in the range of 76–84% as shown in the formation of **2d** and **2e** in 68% and 73% selectivity, respectively. Remarkably, the *N*-unprotected phthalimide **1f** was converted in 71% yield with a selectivity of 80% for the borylated product **2f** in the proximal position, thereby evidencing no catalyst inhibition effect by the unprotected NH imide group. The reaction was compatible with fluorinated groups as shown in the high conversion (85%) of **1g**, leading to the proximal borylated product **2g** in 60% selectivity. Probing the reactivity of *N*-methylisoindolinone and phthalic anhydride resulted in a mixture of unidentified products as it was observed with iodine- and alkyne-containing substrates (Scheme 4 and Chart S1 in the SI). Overall, *click* ligand **I** appears complementary to Xu's ligand **L6** (Fig. 1) in order to perform iridium-catalysed proximal C–H borylation of phthalimides beyond *N*-aryl substitution patterns. Note that proximal iridium-catalysed C–H borylation with larger perylene diimides or 1,2-doubly-fused six-membered rings are known.[88–90]

Moreover, the regio-selectivity of the *click* ligand **I**-controlled iridium-catalysed C–H borylation of phthalimides was unambiguously confirmed by SCXRD performed with the hydroxylated derivatives **4a** and **4f** obtained from oxidative post-functionalizations of **2a** and **2f**, independently, upon treatment with oxone, respectively (Scheme 5).

Furthermore, the *click* ligand-controlled proximal C–H borylation under iridium catalysis was compatible with other useful carbonyl-containing aromatic substrates. Importantly, it was possible to replace *click* ligand **I** by *click* ligand **A**, whose synthesis implies a single step, with equal efficiency in terms of activity and selectivity for the proximal iridium-catalysed C–H borylation of these substrates (Scheme 6). Applying the optimal, iridium-catalysed borylating reaction conditions with *click* ligand **A** to acetophenone (**1h**), methylbenzoate (**1i**) and

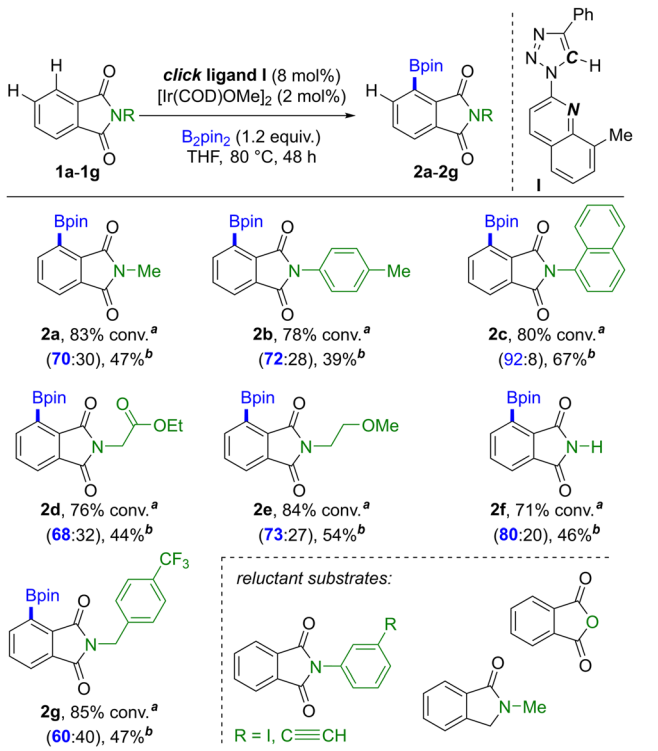

Scheme 4 Substrate scope evaluation of *click* ligand **I**-controlled iridium-catalysed C–H borylation for proximal selectivity with phthalimides. [a] Conversion of **1** and product selectivity in brackets for **2** (**2** : others) were determined by GC analysis using dodecane as an internal standard. [b] Isolated yield as the corresponding boronic acid derivative after purification by silica column chromatography.

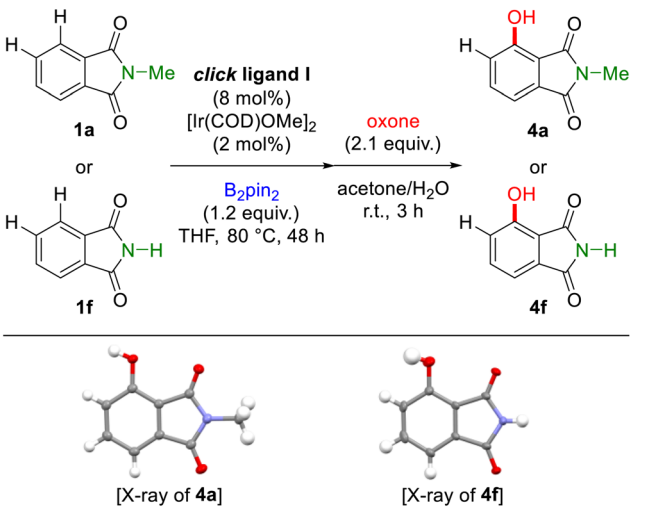

Scheme 5 Sequential iridium-catalysed C–H borylation and oxidative post-functionalization of phthalimides **1a** and **1f** (top) and SCXRD of proximal hydroxylated derivatives **4a** (CCDC 2480986) and **4f** (CCDC 2480987), respectively (ORTEP drawings with thermal ellipsoids at 50% probability, bottom).

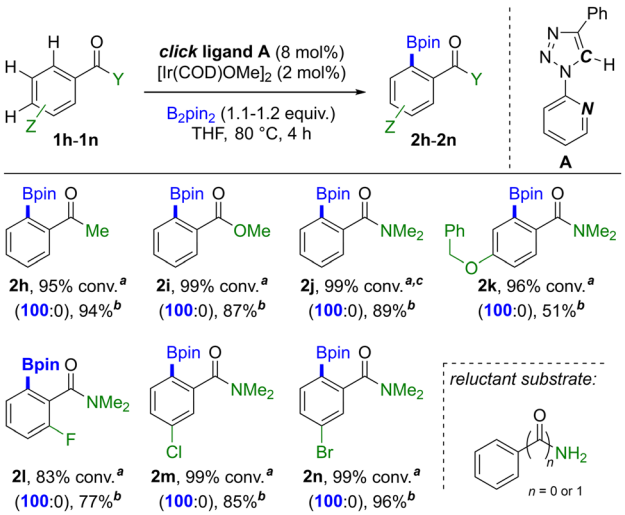

Scheme 6 Substrate scope evaluation of the *click* ligand **A**-controlled iridium-catalyzed C–H borylation for proximal *ortho*-selectivity with carbonyl-containing aromatics. [a] Conversion of **1** and product selectivity in brackets for **2** (**2** : others) were determined by GC analysis using dodecane as an internal standard. [b] Isolated yield after purification by silica column chromatography. [c] 3 hours of reaction time.

N,*N*-dimethylbenzamide (**1j**) as substrates, respectively, led to virtually quantitative conversions and exclusive proximal, *ortho*-selectivity with the corresponding borylated products **2h**, **2i** and **2j** isolated in 87–94% yields in short reaction times of 3–4 hours. The *click* ligand-controlled iridium-catalysed C–H borylation was also tolerant to benzyl ether groups (**2k**), thus indicating that the carbonyl group from the amide is a better directing group than the oxygen from the ether group as further corroborated by the lack of reactivity found for anisole when used as the substrate (Chart S1 in the SI) and without any detectable borylation in the aromatic benzylic site. Moreover, useful halogen functional groups such as fluoride, chloride and bromide were compatible with the catalysis as demonstrated in the quantitative formation of *ortho*-borylated products **2l**, **2m** and **2n** in 77–96% isolated yields. For the case of the *meta*-substituted starting materials **1m** and **1n**, we noted that the reaction did not occur in the C–H bond flanked by the amide and the halide group, but in the most sterically accessible *ortho*-C–H site. The stability of these compounds made possible to isolate them as the corresponding Bpin-containing products.

For comparison purposes, we performed the catalysis for substrates **1h–1j**, respectively, by replacing *click* ligand **A** for Chattopadhyay's **PTY** ligand. In this case, although exclusive *ortho*-selectivity was achieved, the conversions dropped to <60% after 4 hours of the reaction time (see the SI). Overall, the iridium-catalysed C–H borylation of carbonyl-containing substrates using *click* ligands outperforms the current state-of-the-art ligands (Tables S6–S8 in the SI). We also found that the catalysis was not compatible with unfunctionalized, primary benzamide nor aniline (Scheme 6), whilst a mixture of unidentified products was observed when employing methyl

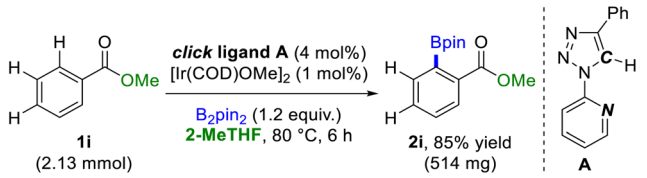

Scheme 7 Scale-up experiment for the *click* ligand **A**-controlled iridium-catalysed C–H borylation of **1j** using 2-MeTHF as the green solvent.

phenyl sulfone as the substrate (Chart S1 in the SI). Chlorobenzene, *N*,*N*-dimethylaniline and L-phenylalanine, respectively, did not react under these reaction conditions (Chart S1 in the SI). Note that statistical mixtures of *meta*- and *para*-borylated products are known to form with iridium catalysts based on classical *N*,*N*-chelating ligands such as **bpy**, **dtbpy** and **phen**.[26–28,50–54] To further demonstrate the applicability of the *click* ligand-controlled iridium-catalysed C–H borylation, a scale-up experiment was carried out with more than 2 mmol of methylbenzoate **1i** (Scheme 7). This time, the catalyst loading was reduced to only 1 mol% of $[Ir(COD)OMe]_2$ and 4 mol% of *click* ligand **A** at 80 °C using 2-MeTHF as the green solvent.[91] After 6 hours, full conversion was observed with exclusive *ortho*-selectivity and the borylated product **2i** was isolated in 85% yield, which corresponds to more than 500 mg.

Postulated nature of the catalytically-active iridium species: role of the solvent and influence of the substrate

In the case of acyclic carbonyl-containing substrates such as acetophenone (**1h**), methylbenzoate (**1i**) and *N*,*N*-dimethylbenzamide (**1j**) (Fig. 3, top), the use of relatively polar and potentially metal-coordinating solvents (THF, 1,4-dioxane or 2-MeTHF) strongly favours the formation of the *ortho*-C–H borylated products **2h–2j** regardless of the nature of *click* ligand **A** or **I** (Fig. 3, top). These findings together with the above-described coordination chemistry studies with *click* ligands (*vide supra*) strongly support the formation of *N*,*C*-chelating bis(boryl)iridium species **Ir-L*** under *operando* conditions, namely excess of B_2pin_2, when using THF as the solvent (Scheme 8). Indeed, *N*,*C*-chelating bis(boryl)iridium **Ir-L*** species, with a vacant site at iridium, should allow the transient coordination of the carbonyl group of the substrate to the iridium prior C–H activation (Fig. 3, top). On the other hand, an apolar non-coordinating solvent such as *p*-xylene afforded, besides the main formation of the *ortho*-borylated product **2h** (95%), non-negligible trace amount of the distally borylated product **3h** at the expenses of a poor conversion below 40% with the *click* ligands (Fig. 3, top). This is rationalized by the fact that *N*,*C*-chelating bis(boryl)iridium **Ir-L*** species are formed under *operando* conditions but in little amounts, thanks to the presence of additional, small quantities of the coordinating COD ligand that may play a similar role as the THF solvent in transiently stabilizing catalytically productive iridium intermediates. In this case, with an apolar solvent, *N*,*N*-chelating tris(boryl)iridium species **Ir′-L***

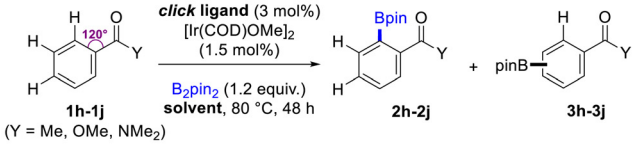

click ligand	solvent	conv. **1**	ratio **2**:**3**
A or **I**	THF or 1,4-dioxane	99%	100:0
A or **I**	*p*-xylene	<40%	95:5

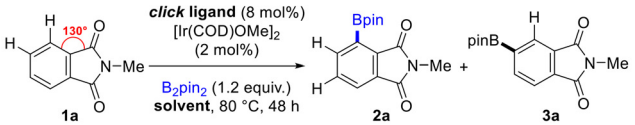

click ligand	solvent	conv. **1**	ratio **2**:**3**
A	THF or 1,4-dioxane	≈80%	33:63
A	*p*-xylene	<30%	0:100
I	THF or 1,4-dioxane	83-85%	71:29
I	*p*-xylene	<30%	0:100

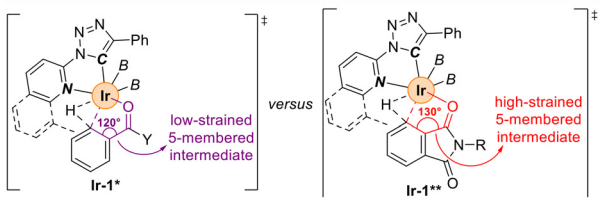

Fig. 3 Comparative study of the iridium-catalysed C–H borylation of acyclic carbonyl-containing aromatics (top) and bicyclic phthalimide (middle) with different *click* ligands (**A** and **I**) and solvents of different natures: polar, coordinating *versus* apolar, non-coordinating, and plausible transition state intermediates for the iridium-mediated C–H activation step depending on the nature of the carbonyl-containing aromatic substrate (bottom). *B* = (boron)pinacolato.

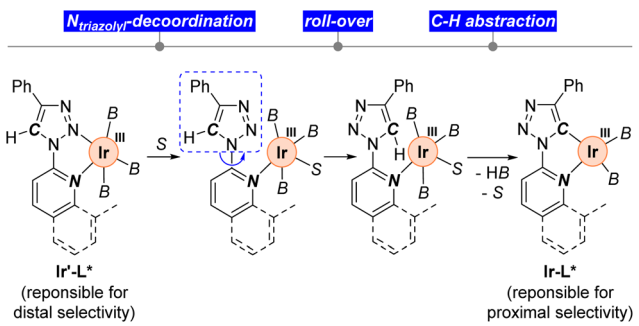

Scheme 8 Postulated mechanism for both solvent- and B_2pin_2-mediated *click* ligand C–H abstraction under *operando* conditions towards the formation of *N*,*C*-chelating bis(boryl)iridium species **Ir-L***. *B* = (boron)pinacolato and *S* = THF or COD.

(Scheme 8), responsible for the non-directed C–H borylation leading to the products **3h–3j**, are also formed but to a much less extent or either they are less reactive than the *N*,*C*-chelated species **Ir-L***. Due to the fact that the carbonyl-containing substrates feature a standard 120° angle between the carbonyl group and the *ortho*-C–H bond (Fig. 3, top), it is reasonable to postulate that the reaction intermediates responsible for *ortho*-selectivity that are also involved in the coordination of the carbonyl group of the substrate to the iridium are rather accessible (**Ir-1***, Fig. 3, bottom), which makes these reactions relatively fast (3–4 hours with 2 mol% of the iridium dimer pre-catalyst, Scheme 6).

Alternatively, when considering phthalimides, which display a larger *ca.* 130° angle between the carbonyl group and the proximal C–H bond (Fig. 3, middle), the difference of reactivity is remarkable when comparing *click* ligands **A** and **I** in the presence of polar, metal-coordinating solvents (Fig. 3, middle). Although both *click* ligands are expected to form *N*,*C*-chelated bis(boryl)iridium species **Ir-L*** (*vide supra*), ligand **I** appears to be more suitable than **A** to further accommodate the reaction intermediates responsible for carbonyl-directed proximal C–H borylation with **2a**, forming in >70% yield. The expected highly strained intermediates associated with the proximal C–H borylation of phthalimides (**Ir-1****, Fig. 3, bottom) have also to compete with the likely presence of small amounts of *N*,*N*-chelating tris(boryl)iridium species **Ir′-L*** (Scheme 8) responsible for distal selectivity (**3a**). This is further indirectly corroborated by the fact that *click* ligands **A** and **I** exclusively lead to non-directed distal C–H borylation when using an apolar, non-coordinating solvent such as *p*-xylene yet with low conversion below 30% (Fig. 3, middle). Consequently, *click* ligands can be considered as ambiphiles as they can switch from neutral *N*,*N*-chelators to anionic *N*,*C*-chelators to iridium depending on the nature of the solvent and the reaction conditions.

In short, all these observations are compelling with the fact that THF or COD are at the origin for enabling eventual decoordination at **Ir′-L*** species of the triazolyl nitrogen atom from the *click* ligand followed by roll-over at iridium.[92,93] Then, C–H abstraction at the triazolyl core takes place either *via* sigma-bond metathesis or *via* oxidative addition at iridium; in both cases, HBpin is released with additional stabilization by THF or COD ligands. In this manner, the *N*,*C*-chelated bis(boryl)iridium species **Ir-L*** might form with *click* ligands under *operando* conditions (Scheme 8), being them responsible for the observed proximal C–H bond borylation selectivity. Furthermore, and supported by the substrate scope evaluation (*vide supra*), the anionic *click* ligands formed under *operando* conditions led to very active iridium species for substrate-directed *ortho*-C–H borylation and underscores the challenge to perform proximal C–H borylation with more sterically-demanding phthalimides compared to acyclic carbonyl-containing substrates.

Mechanistic considerations of the iridium-catalysed C–H borylation with *click* ligands

As control experiments, we noted that *N*-phenylisoindoline and carbonyl-free aromatics such as ethylbenzene did not

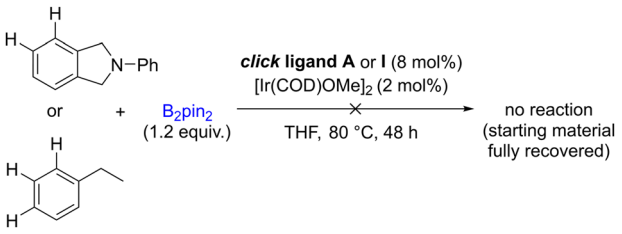

Scheme 9 Control experiments of the unsuccessful iridium-catalysed C–H borylation of carbonyl-free substrates using *click* ligands.

undergo iridium-catalysed C–H borylation using *click* ligands **A** or **I** (Scheme 9). These findings strongly suggest that substrate coordination to the iridium *via* the carbonyl group is a key event for enabling the highly efficient, *ortho*-C–H borylation in carbonyl-containing aromatic substrates, which is also in line with the observations encountered during the scope evaluation (*vide supra*).[94,95]

To assess whether the C–H bond activation step is the rate-determining one, kinetic isotope effect (KIE) experiments were performed using the benzamide starting material (**1j**) and the penta-deuterated one (**1j**-d_5), respectively (Scheme 10).[96] From the two parallel experiments, a relatively high KIE of 2.13 was found in the initial hour of the catalysis (Fig. S9–S12 in the SI). The intermolecular competition experiment was less conclusive to analyze because of signals overlapping in the ^{1}H NMR spectrum yet an estimated KIE value in the range 1.6–2.4 was established (Fig. S13 and S14 in the SI).

In order to further study the reaction mechanism operating, in-depth kinetic studies were performed by performing both Blackmond's reaction progress kinetic analysis (RPKA) and Bures' visual kinetic analysis (VKA) to the iridium-catalysed C–H borylation of *N*-methylphthalimide (**1a**) in the presence of *click* ligand **I**.[97,98] Although the reaction was not trivial to monitor due to the presence of non-negligible amounts of the distal borylated product **3a** and bis-borylated side-products after 8 hours, acceptable curve fittings were obtained in the initial moments of the catalysis (Fig. S15–S29 in the SI). As a result, the reaction was found first order in iridium and in the substrate. The fact that the reaction order in B_2pin_2 was also one likely indicates that isomerization at the C–H activated

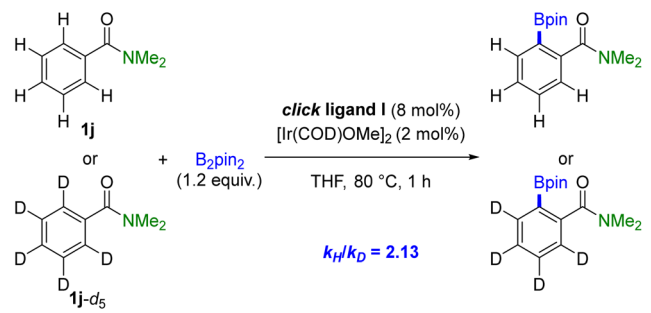

Scheme 10 Kinetic isotope effect (KIE) determined from parallel reactions of substrates **1j** and **1j**-d_5.

iridium(v) complex **Ir-b** (Scheme 11) might be turnover-limiting.[99,100] These observations together with the KIE studies (*vide supra*) indicate that both C–H activation (**Ir-a** → **Ir-b**, Scheme 11) and isomerization at the C–H-activated iridium(v) complex **Ir-b** (Scheme 11) may have similar energetic barriers for their respective transition states, being not possible to differentiate at this stage which one is turnover-limiting. Further kinetic studies indicated that product inhibition instead of catalyst deactivation was taking place, which might account for the formation of bis-borylated side-products.

Considering all the above-stated findings and previous reports from the literature,[38–49] a plausible reaction mechanism is proposed in Scheme 11 for the iridium-catalysed C–H borylation using *click* ligands **L***. Besides the fact that solvent plays a major role (*vide supra*), it is relevant to note that some *click* ligands such as **C–F** may give rise to tris(boryl)iridium species responsible for distal C–H borylation either *via N,N*-chelation or *via* two-fold monodentate coordination (Scheme 11, top). The other *click* ligands, and in particular **A** and **I**, undergo iridacycle

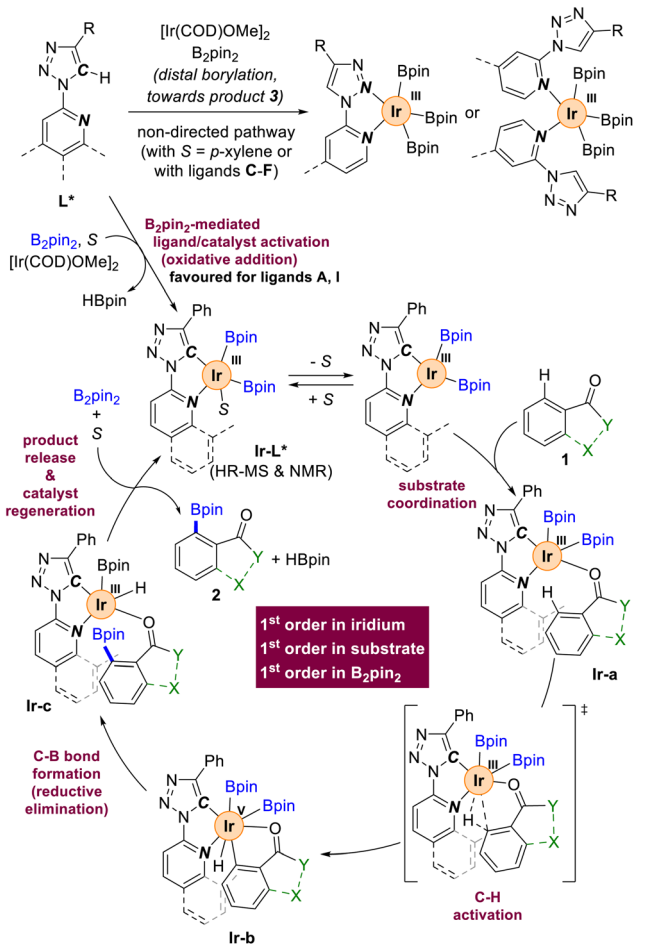

Scheme 11 Postulated reaction mechanism for proximal iridium-catalysed C–H borylation of carbonyl-containing aromatics using *click* ligands **A** and **I** and summary of kinetic studies with *N*-methylphthalimide **1a** (framed). X = H or CO; Y = NR_2, R, or OR; *S* = THF or COD.

formation upon abstraction of the triazolyl C–H bond and oxidative addition in the presence of excess of B_2pin_2, resulting in the formation of **Ir-L*** species that can be further stabilized by transient coordination of THF or COD to iridium as evidenced by NMR and HR-MS studies (*vide supra*, Scheme 11). Upon decoordination of the COD ligand or ligand exchange with the THF solvent, the substrate (**1**) coordinates to the iridium *via* the carbonyl group (**Ir-a**) and brings the proximal C–H bond at close proximity. Next, iridium-mediated C–H activation takes place, leading to iridium(v) species (**Ir-b**). Finally, reductive elimination at iridium allows C–B bond formation (**Ir-c**), leading to the *ortho*-borylated product (**2**), while B_2pin_2 regenerates the catalytically active iridium species. Note that we attempted the iridium-catalysed C–H borylation of *N*-methylphthalimide **1a** with the preformed **Ir-A** species, leading to a similar regioselectivity as obtained with the *ex situ* approach yet with a low conversion likely due to the low stability of the **Ir-A** species (Scheme S1 in the SI).

Conclusions

In summary, we have reported the original action mode of *click* ligands **L***, which are straightforward to prepare *via* sustainable copper-catalysed **CuAAC** *click* chemistry, in *ortho*-selective iridium-catalysed C–H bond borylation of synthetically useful carbonyl-containing substrates including phthalimides with high functional group tolerance. In contrast to previously reported ligands that contain heavy heteroatoms such as As, B, P, Si, F or S,[36–54] the *click* ligands herein developed rely on C, H, and N atoms, are air-stable and are easy to fine tune at different positions while leading to a unique co-planarity between the triazolyl core and the aromatic substituents. Such pre-organization together with the slight acidity of the triazolyl C–H bond enables the *click* ligands to behave as anionic ones, enabling *L*,*X*-chelation to iridium exclusively under *operando* conditions, namely an excess of the borylating agent with respect to the ligand/iridium loading with a polar-coordinating solvent (*i.e.* THF, 1,4-dioxane or bio-sourced 2-MeTHF), as supported by a number of experimental studies (NMR, HR-MS, and kinetics). This contribution highlights that ligands that contain C–H bonds close to 2-pyridyl motifs, which are omnipresent in iridium-catalysed C–H bond borylations, can potentially undergo C–H abstraction switching from neutral to anionic under catalytically relevant conditions, thereby raising questions about previously postulated reaction mechanisms for *ortho*-selectivity in iridium-catalysed C–H borylations.[51–53]

Importantly, the overlooked additional role of both solvent and B_2pin_2 in enabling ligand modification under *operando* conditions is demonstrated, and such an action mode might be considered in the future design of more active and selective iridium catalysts for C–H bond borylations. Beyond solvent-controlled selective catalysis,[101–105] understanding the real nature of the active species under *operando* conditions and the precise chemical structure of the ligand should allow the rational design of a more powerful, future generation of catalysts for selective C–H borylation. Furthermore, structural ligand modification during metal-catalysed C–H bond functionalization beyond iridium catalysts could represent an interesting opportunity for the advancement of more atom-economical and efficient chemical processes.

Author contributions

Conceptualization: M. A. and R. G.-D.; data curation: V. D. and R. G.-D.; formal analysis: V. D., T. R., M. A. and R. G.-D.; supervision: S. D., M. A. and R. G.-D.; funding acquisition: S. D., M. A. and R. G.-D.; validation, visualization and investigation: V. D. and R. G.-D.; methodology: V. D. and T. R.; writing – original draft: V. D. and R. G.-D.; project administration: S. D., M. A. and R. G.-D.; writing – review and editing: V. D. and R. G.-D.

Conflicts of interest

There are no conflicts to declare.

Data availability

The dataset supporting this article has been uploaded as part of the supplementary information (SI). Supplementary information: experimental details for the preparation and characterization of *click* ligands, details of *operando* coordination chemistry to iridium (NMR and HR-MS), catalysis, kinetics, and details on isolation and characterization of the reaction products. See DOI: **https://doi.org/10.1039/d6qi00270f**.

CCDC 2480983 (**A**), 2480984 (**K**), 2480985 (precursor of **N**), 2480986 (**4a**) and 2480987 (**4f**) contain the supplementary crystallographic data for this paper.[106a–e]

Acknowledgements

The CNRS, the University of Rennes and Ministère de l'Enseignement supérieur et de la Recherche (PhD grant to VD) are acknowledged for financial support. Jonathan Trouvé is acknowledged for the initial experimentation, and Elisa Travers and Kamil Kupietz are acknowledged for the synthesis of one starting material and for obtaining a single crystal suitable for X-ray diffraction studies, respectively.

References

1 *Handbook of CH-Functionalization*, ed. D. Maiti, Wiley-VCH, Weinheim, 2022.
2 G. Meng, N. Y. S. Lam, E. L. Lucas, T. G. Saint-Denis, P. Verma, N. Chekshin and J.-Q. Yu, Achieving Site-

Selectivity for C–H Activation Processes Based on Distance and Geometry: A Carpenter's Approach, *J. Am. Chem. Soc.*, 2020, **142**, 10571–10591.

3 T. Rogge, N. Kaplaneris, N. Chatani, J. Kim, S. Chang, B. Punji, L. L. Schafer, D. G. Musaev, J. Wencel-Delord, C. A. Roberts, R. Sarpong, Z. E. Wilson, M. A. Brimble, M. J. Johansson and L. Ackermann, C–H activation, *Nat. Rev. Methods Primers*, 2021, **1**, 43.

4 J. F. Hartwig, Evolution of C–H Bond Functionalization from Methane to Methodology, *J. Am. Chem. Soc.*, 2016, **138**, 2–24.

5 S. K. Sinha, S. Guin, S. Maiti, J. P. Biswas, S. Pore and D. Maiti, Toolbox for Distal C–H Bond Functionalizations in Organic Molecules, *Chem. Rev.*, 2022, **122**, 5682–5841.

6 I. A. Stepek and K. Itami, Recent Advances in C–H Activation for the Synthesis of π-Extended Materials, *ACS Mater. Lett.*, 2020, **2**, 951–974.

7 T. Dalton, T. Faber and F. Glorius, C–H Activation: Toward Sus-tainability and Applications, *ACS Cent. Sci.*, 2021, **7**, 245–261.

8 L. Guillemard, N. Kaplaneris, L. Ackermann and M. J. Johansson, Late-stage C–H functionalization offers new opportunities in drug discovery, *Nat. Rev. Chem.*, 2021, **5**, 522–545.

9 T. Cernak, K. D. Dykstra, S. Tyagarajan, P. Vachalb and S. W. Krska, The medicinal chemist's toolbox for late stage functionalization of drug-like molecules, *Chem. Soc. Rev.*, 2016, **45**, 546–576.

10 J. F. Hartwig and M. A. Larsen, Undirected, Homogeneous C–H Bond Functonalization: Challenges and Opportunities, *ACS Cent. Sci.*, 2016, **2**, 281–292.

11 J. H. Docherty, T. M. Lister, G. McArthur, M. T. Findlay, P. Domingo-Legarda, J. Kenyon, S. Choudhary and I. Larrosa, Transition-Metal-Catalyzed C–H Bond Activation for the Formation of C–C Bonds in Complex Molecules, *Chem. Rev.*, 2023, **123**, 7692–7760.

12 N. Della Ca′, M. Fontana, E. Motti and M. Catellani, Pd/Norbornene: A Winning Combination for Selective Aromatic Functionalization via C–H Bond Activation, *Acc. Chem. Res.*, 2016, **49**, 1389–1400.

13 J. Takagi, K. Sato, J. F. Hartwig, T. Ishiyama and N. Miyaura, Iridium-catalyzed C–H coupling reaction of heteroaromatic compounds with bis(pinacolato)diboron: regioselective syn-thesis of heteroarylboronates, *Tetrahedron Lett.*, 2002, **43**, 5649–5651.

14 T. M. Boller, J. M. Murphy, M. Hapke, T. Ishiyama, N. Miyaura and J. F. Hartwig, Mechanism of the Mild Functionalization of Arenes by Diboron Reagents Catalyzed by Iridium Complexes. Intermediacy and Chemistry of Bipyridine-Ligated Iridium Trisboryl Complexes, *J. Am. Chem. Soc.*, 2005, **127**, 14263–14278.

15 T. Ishiyama, J. Takagi, K. Ishida, N. Miyaura, N. R. Anastasi and J. F. Hartwig, Mild Iridium-Catalyzed Borylation of Arenes. High Turnover Numbers, Room Temperature Reactions, and Isolation of a Potential Intermediate, *J. Am. Chem. Soc.*, 2002, **124**, 390–391.

16 T. Ishiyama, Y. Nobuta, J. F. Hartwig and N. Miyaura, Room temperature borylation of arenes and heteroarenes using stoichiometric amounts of pinacolborane catalyzed by iridium complexes in an inert solvent, *Chem. Commun.*, 2003, 2924–2925.

17 T. Ishiyama, J. Takagi, J. F. Hartwig and N. Miyaura, A Stoichiometric Aromatic C–H Borylation Catalyzed by Iridium(I)/2,2′-Bipyridine Complexes at Room Temperature, *Angew. Chem., Int. Ed.*, 2002, **41**, 3056–3058.

18 Y. Saito, Y. Segawa and K. Itami, para-C–H Borylation of Benzene Derivatives by a Bulky Iridium Catalyst, *J. Am. Chem. Soc.*, 2015, **137**, 5193–5198.

19 R. Bisht, C. Haldar, M. M. M. Hassan, M. E. Hoque, J. Chaturvedi and B. Chattopadhyay, Metal-catalysed C–H bond activation and borylation, *Chem. Soc. Rev.*, 2022, **51**, 5042–5100.

20 M. M. M. Hassan, S. Guria, S. Dey, J. Das and B. Chattopadhyay, Transition metal–catalyzed remote C—H borylation: An emerging synthetic tool, *Sci. Adv.*, 2023, **9**, eadg3311.

21 I. F. Yu, J. W. Wilson and J. F. Hartwig, Transition-Metal-Catalyzed Silylation and Borylation of C–H Bonds for the Synthesis and Functionalization of Complex Molecules, *Chem. Rev.*, 2023, **123**, 11619–11663.

22 O. Kuleshova, S. Asako and L. Ilies, Ligand-Enabled, Iridium-Catalyzed ortho-Borylation of Fluoroarenes, *ACS Catal.*, 2021, **11**, 5968–5973.

23 *Boronic Acids, Preparation, Applications in Organic Synthesis*, ed. D. G. Hall, Wiley-VCH, Weinheim, 2011.

24 E. C. Neeve, S. J. Geier, I. A. I. Mkhalid, S. A. Westcott and T. B. Marder, Diboron(4) Compounds: From Structural Curiosity to Synthetic Workhorse, *Chem. Rev.*, 2016, **116**, 9091–9161.

25 M. Wang and Z. Shi, Methodologies and Strategies for Selective Borylation of C–Het and C–C Bonds, *Chem. Rev.*, 2020, **120**, 7348–7398.

26 Y. Kuninobu, H. Ida, M. Nishi and M. Kanai, A meta-selective C–H borylation directed by a secondary interaction between ligand and substrate, *Nat. Chem.*, 2015, **7**, 712–717.

27 H. J. Davis, M. T. Mihai and R. J. Phipps, Ion Pair-Directed Regio-control in Transition-Metal Catalysis: A Meta-Selective C–H Borylation of Aromatic Quaternary Ammonium Salts, *J. Am. Chem. Soc.*, 2016, **138**, 12759–12762.

28 L. Yang, K. Semba and Y. Nakao, para-Selective C–H Borylation of (Hetero)Arenes by Cooperative Iridium/Aluminum Catalysis, *Angew. Chem., Int. Ed.*, 2017, **56**, 4853–4857.

29 M. E. Hoque, R. Bisht, C. Haldar and B. Chattopadhyay, Non-covalent Interactions in Ir-Catalyzed C–H Activation: L-Shaped Ligand for Para-Selective Borylation of Aromatic Esters, *J. Am. Chem. Soc.*, 2017, **139**, 7745–7748.

30 J. R. Montero Bastidas, T. J. Oleskey, S. L. Miller, M. R. Smith and R. E. Maleczka, Para-Selective, Iridium-Catalyzed C–H Borylations of Sulfated Phenols, Benzyl

Alcohols, and Anilines Directed by Ion-Pair Electrostatic Interactions, *J. Am. Chem. Soc.*, 2019, **141**, 15483–15487.

31 B. Chattopadhyay, J. E. Dannatt, I. L. Andujar-De Sanctis, K. A. Gore, R. E. Maleczka, D. A. Singleton and M. R. Smith, Ir-Catalyzed ortho-Borylation of Phenols Directed by Substrate–Ligand Electrostatic Interactions: A Combined Experimental/in Silico Strategy for Optimizing Weak Interactions, *J. Am. Chem. Soc.*, 2017, **139**, 7864–7871.

32 B. Ramadoss, Y. Jin, S. Asako and L. Ilies, Remote steric control for undirected meta-selective C–H activation of arenes, *Science*, 2022, **375**, 658–663.

33 S. Lu, T. Zheng, J. Ma, Z. Deng, S. Qin, Y. Chen and Y. Liang, para-Selective C–H Borylation of Aromatic Quaternary Ammonium and Phosphonium Salts, *Angew. Chem., Int. Ed.*, 2022, **61**, e202201285.

34 J. Trouvé, P. Zardi, S. Al-Shehimy, T. Roisnel and R. Gramage-Doria, Enzyme-like Supramolecular Iridium Catalysis Enabling C–H Bond Borylation of Pyridines with meta-Selectivity, *Angew. Chem., Int. Ed.*, 2021, **60**, 18006–18013.

35 J. Trouvé, P. Rajeshwaran, M. Tomasini, A. Perennes, T. Roisnel, A. Poater and R. Gramage-Doria, Fast and Selective β-C–H Borylation of N-Heterocycles with a Supramolecular Iridium Catalyst: Circumventing Deactivation Pathways and Mechanistic Insights, *ACS Catal.*, 2023, **13**, 7715–7729.

36 T. Ishiyama, H. Isou, T. Kikuchia and N. Miyaura, Ortho-C–H borylation of benzoate esters with bis(pinacolato) diboron catalyzed by iridium–phosphine complexes, *Chem. Commun.*, 2010, **46**, 159–161.

37 H. Itoh, T. Kikuchi, T. Ishiyama and N. Miyaura, Iridium-catalyzed ortho-C–H Borylation of Aryl Ketones with Bis (pinacolato)diboron, *Chem. Lett.*, 2011, **40**, 1007–1008.

38 B. Ghaffari, S. M. Preshlock, D. L. Plattner, R. J. Staples, P. E. Maligres, S. W. Krska, R. E. Maleczka Jr. and M. R. Smith III, Silyl Phosphorus and Nitrogen Donor Chelates for Homogeneous Ortho Borylation Catalysis, *J. Am. Chem. Soc.*, 2014, **136**, 14345–14348.

39 J. E. Dannatt, A. Yadav, M. R. Smith III and R. E. Maleczka Jr., Amide directed iridium C(sp^3)–H borylation catalysis with high N-methyl selectivity, *Tetrahedron Lett.*, 2022, **109**, 132578.

40 A. C. O'Connell, P. A. Mansour, R. E. Maleczka Jr. and M. R. Smith III, Regiochemical Switching in Ir-Catalyzed C–H Borylation by Altering Ligand Loadings of N,B-Type Diboron Species, *Org. Lett.*, 2023, **25**, 8057–8061.

41 G. Wang, L. Liu, H. Wang, Y.-S. Ding, J. Zhou, S. Mao and P. Li, N,B-Bidentate Boryl Ligand-Supported Iridium Catalyst for Efficient Functional-Group-Directed C–H Borylation, *J. Am. Chem. Soc.*, 2017, **139**, 91–94.

42 X. Zou, H. Zhao, Y. Li, Q. Gao, Z. Ke and S. Xu, Chiral Bidentate Boryl Ligand Enabled Iridium-Catalyzed Asymmetric C(sp^2)–H Borylation of Diarylmethylamines, *J. Am. Chem. Soc.*, 2019, **141**, 5334–5342.

43 C. Liu, C. Xia, S.-Y. Song and S. Xu, Ether-Directed Enantioselec-tive C(sp2)–H Borylation for the Synthesis of Axially Chiral Biaryls, *Org. Lett.*, 2025, **27**, 4232–4237.

44 H. Zhao, C.-Y. Zhao, L. Chen, C. Xia, X. Hong and S. Xu, Aryl Chloride-Directed Enantioselective C(sp^2)-H Borylation Enabled by Iridium Catalysis, *J. Am. Chem. Soc.*, 2023, **145**, 25214–25221.

45 S.-Y. Song, X. Zhou, Z. Ke and S. Xu, Synthesis of Chiral Sulfoximines via Iridium-Catalyzed Regio- and Enantioselective C–H Borylation: A Remarkable Sidearm Effect of Ligand, *Angew. Chem., Int. Ed.*, 2023, **62**, e202217130.

46 S.-Y. Song, Y. Li, Z. Ke and S. Xu, Iridium-Catalyzed Enantioselective C–H Borylation of Diarylphosphinates, *ACS Catal.*, 2021, **11**, 13445–13451.

47 M. E. Hoque, M. M. M. Hassan and B. Chattopadhyay, Remarkably Efficient Iridium Catalysts for Directed C(sp^2)–H and C(sp^3)–H Borylation of Diverse Classes of Substrates, *J. Am. Chem. Soc.*, 2021, **143**, 5022–5037.

48 J. M. Zakis, A. M. Messinis, L. Ackermann, T. Smejkal and J. Wencel-Delord, Air-Stable Bis-Cyclometallated Iridium Catalysts for Ortho-Directed C(sp^2)–H Borylation, *Adv. Synth. Catal.*, 2024, **366**, 2292–2304.

49 J. M. Zakis, R. A. Lipina, S. Bell, S. R. Williams, M. Mathis, M. J. Johansson, J. Wencel-Delord and T. Smejkal, High-Throughput Enabled Iridium-Catalyzed C–H Borylation Platform for Late-Stage Functionalization, *ACS Catal.*, 2025, **15**, 3525–3534.

50 S. Kawamorita, H. Ohmiya, K. Hara, A. Fukuoka and M. Sawamura, Directed Ortho Borylation of Functionalized Arenes Catalyzed by a Silica-Supported Compact Phosphine–Iridium System, *J. Am. Chem. Soc.*, 2009, **131**, 5058–5059.

51 D. Marcos-Atanes, C. Vidal, C. D. Navo, F. Peccati, G. Jiménez-Osés and J. L. Mascarenas, Iridium-Catalyzed ortho-Selective Borylation of Aromatic Amides Enabled by 5-Trifluoromethylated Bipyridine Ligands, *Angew. Chem., Int. Ed.*, 2023, **62**, e202214510.

52 S.-T. Bai, C. B. Bheeter and J. N. H. Reek, Hydrogen Bond Directed ortho-Selective C–H Borylation of Secondary Aromatic Amides, *Angew. Chem., Int. Ed.*, 2019, **58**, 13039–13043.

53 H. L. Li, Y. Kuninobu and M. Kanai, Lewis Acid–Base Interaction-Controlled ortho-Selective C–H Borylation of Aryl Sulfides, *Angew. Chem., Int. Ed.*, 2017, **56**, 1495–1499.

54 J. Trouvé, V. Delahaye, M. Tomasini, P. Rajeshwaran, T. Roisnel, A. Poater and R. Gramage-Doria, Repurposing a supramolecular iridium catalyst via secondary Zn···O═C weak interactions between the ligand and substrate leads to ortho-selective C(sp^2)–H borylation of benzamides with unusual kinetics, *Chem. Sci.*, 2024, **15**, 11794–11806.

55 V. V. Rostovtsev, L. G. Green, V. V. Fokin and K. B. Sharpless, A Stepwise Huisgen Cycloaddition Process: Copper(I)-Catalyzed Regioselective "Ligation" of Azides and Terminal Alkynes, *Angew. Chem., Int. Ed.*, 2002, **41**, 2596–2599.

56 M. Meldal and C. W. Tornøe, Cu-Catalyzed Azide–Alkyne Cycloaddition, *Chem. Rev.*, 2008, **108**, 2952–3015.

57 H. C. Kolb, M. G. Finn and K. B. Sharpless, Click Chemistry: Diverse Chemical Function from a Few Good Reactions, *Angew. Chem., Int. Ed.*, 2001, **40**, 2004–2021.

58 J. D. Crowley and E. L. Gavey, Use of di-1,4-substituted-1,2,3-triazole "click" ligands to self-assemble dipalladium(II) coordinatively saturated, quadruply stranded helicate cages, *Dalton Trans.*, 2010, **39**, 4035–4037.
59 M. L. Gower and J. D. Crowley, Self-assembly of silver(I) metallomacrocycles using unsupported 1,4-substituted-1,2,3-triazole "click" ligands, *Dalton Trans.*, 2010, **39**, 2371–2378.
60 T. L. Mindt, H. Struthers, L. Brans, T. Anguelov, C. Schweinsberg, V. Maes, D. Tourwé and R. Schibli, "Click to Chelate": Synthesis and Installation of Metal Chelates into Biomolecules in a Single Step, *J. Am. Chem. Soc.*, 2006, **128**, 15096–15097.
61 R. M. Meudtner, M. Ostermeier, R. Goddard, C. Limberg and S. Hecht, Multifunctional "Clickates" as Versatile Extended Heteroaromatic Building Blocks: Efficient Synthesis via Click Chemistry, Conformational Preferences, and Metal Coordination, *Chem. – Eur. J.*, 2007, **13**, 9834–9840.
62 Y. Hua and A. H. Flood, Click chemistry generates privileged CH hydrogen-bonding triazoles: the latest addition to anion supramolecular chemistry, *Chem. Soc. Rev.*, 2010, **39**, 1262–1271.
63 M. Zurro, S. Asmus, J. Bamberger, S. Beckendorf and O. G. Mancheno, Chiral Triazoles in Anion-Binding Catalysis: New Entry to Enantioselective Reissert-Type Reactions, *Chem. – Eur. J.*, 2016, **22**, 3785–3793.
64 K. Shen, Y. Fu, J.-N. Li, L. Liu and Q.-X. Guo, What are the pKa values of C–H bonds in aromatic heterocyclic compounds in DMSO?, *Tetrahedron*, 2007, **63**, 1568–1576.
65 F. G. Bordwell, Equilibrium acidities in dimethyl sulfoxide solution, *Acc. Chem. Res.*, 1988, **21**, 456–463.
66 E. J. Yoo, M. Ahlquist, S. H. Kim, I. Bae, V. V. Fokin, K. B. Sharpless and S. Chang, Copper-Catalyzed Synthesis of N-Sulfonyl-1,2,3-triazoles: Controlling Selectivity, *Angew. Chem., Int. Ed.*, 2007, **46**, 1730–1173.
67 M. Moreno-Latorre, M. C. de la Torre, H. Gornitzka, C. Hemmert and M. A. Sierra, Mono- and Dinuclear 1-(2-Pyridyl)-4-phenyl-1,2,3-triazole-Based Ir(III) and Rh(III) Complexes, *Organometallics*, 2024, **43**, 1128–1136.
68 Y.-C. Yuan, C. Bruneau and R. Gramage-Doria, Merging Transition-Metal Catalysis with Phthalimides: A New Entry to Useful Building Blocks, *Synthesis*, 2018, 4216–4228.
69 Y. Wu and W. Zhu, Organic sensitizers from D–π–A to D–A–π–A: effect of the internal electron-withdrawing units on molecular absorption, energy levels and photovoltaic performances, *Chem. Soc. Rev.*, 2013, **42**, 2039–2058.
70 A. Pulido, L. Chen, T. Kaczorowski, D. Holden, M. A. Little, S. Y. Chong, B. J. Slater, D. P. McMahon, B. Bonillo, C. J. Stackhouse, A. Stephenson, C. M. Kane, R. Clowes, T. Hasell, A. I. Cooper and G. M. Day, Functional materials discovery using energy–structure–function maps, *Nature*, 2017, **543**, 657–664.
71 X. Guo, F. S. Kim, S. A. Jenekhe and M. D. Watson, Phthalimide-Based Polymers for High Performance Organic Thin-Film Transistors, *J. Am. Chem. Soc.*, 2009, **131**, 7206–7207.
72 G. E. Winter, D. L. Buckley, J. Paulk, J. M. Roberts, A. Souza, S. Dhe-Paganon and J. E. Bradner, Phthalimide conjugation as a strategy for in vivo target protein degradation, *Science*, 2015, **348**, 1376–1381.
73 H. Zhao, L. Chen, C. Xia and S. Xu, Enantioselective C–H Borylation for the Synthesis of Axially Chiral N-Aryl Phthalimides, *Asian J. Org. Chem.*, 2023, **12**, e202200695.
74 M. T. Findlay, P. Domingo-Legarda, G. McArthur, A. Yena and I. Larrosa, Catalysis with cycloruthenated complexes, *Chem. Sci.*, 2022, **13**, 3335–3362.
75 N. Y. S. Lam, Z. Fan, K. Wu, H. S. Park, S. Y. Shim, D. A. Strassfeld and J.-Q. Yu, Empirical Guidelines for the Development of Remote Directing Templates through Quantitative and Experimental Analyses, *J. Am. Chem. Soc.*, 2022, **144**, 2793–2803.
76 K. Barral, A. D. Moorhouse and J. E. Moses, Efficient Conversion of Aromatic Amines into Azides: A One-Pot Synthesis of Triazole Linkages, *Org. Lett.*, 2007, **9**, 1809–1811.
77 S. Liu, D. Lentz and C. C. Tzschucke, Conversion of Pyridine N-Oxides to Tetrazolopyridines, *J. Org. Chem.*, 2014, **79**, 3249–3254.
78 S. Jindabot, K. Teerachanan, P. Thongkam, S. Kiatisevi, T. Khamnaen, P. Phiriyawirut, S. Charoenchaidet, T. Sooksimuang, P. Kongsaeree and P. Sangtrirutnugul, Palladium(II) complexes featuring bidentate pyridine–triazole ligands: Synthesis, structures, and catalytic activities for Suzuki–Miyaura coupling reactions, *J. Organomet. Chem.*, 2014, **750**, 35–40.
79 P. Li, J. Zhao, C. Xia and F. Li, The development of carbene-stabilized N–O radical coupling strategy in metal-free regioselective C–H azidation of quinoline N-oxides, *Org. Chem. Front.*, 2015, **2**, 1313–1317.
80 Y. Zhang, S. Zhang, G. Xu, M. Li, C. Tang and W. Fan, Cu-Catalyzed carbamoylation versus amination of quinoline N-oxide with formamides, *Org. Biomol. Chem.*, 2019, **17**, 309–314.
81 M. B. Harisha, M. Nagaraj, S. Muthusubramanian and N. Bhuvanesh, Base free regioselective synthesis of α-triazolylazine derivatives, *RSC Adv.*, 2016, **6**, 58118–58124.
82 B. Chattopadhyay, C. I. R. Vera, S. Chuprakov and V. Gevorgyan, Fused tetrazoles as azide surrogates in click reaction: efficient synthesis of N-heterocycle-substituted 1,2,3-triazoles, *Org. Lett.*, 2010, **12**, 2166–2169.
83 G. S. Sontakke, R. K. Shukla and M. R. Volla, Deoxygenative C2-heteroarylation of quinoline N-oxides: facile access to α-triazolylquinolines, *Beilstein J. Org. Chem.*, 2021, **17**, 485–493.
84 ^{1}H–^{1}H NOESY experiments performed with *click* ligand **A** remained inconclusive due to overlapping of key proton signals.

85 P. Buchgraber, M. M. Domostoj, B. Scheiper, C. Wirtz, R. Mynott, J. Rust and A. Fürstner, Synthesis-driven mapping of the dictyodendrin alkaloids, *Tetrahedron*, 2009, **65**, 6519–6534.
86 K. A. D'Angelo, C. La, B. Kotecki, J. W. Wilson, C. Karmel, R. Swiatowiec, N. P. Tu, S. Shekhar and J. F. Hartwig, An Air-Stable, Single-Component Iridium Precatalyst for the Borylation of C–H Bonds on Large to Miniaturized Scales, *J. Am. Chem. Soc.*, 2024, **146**, 32717–32729.
87 S. Han, K. C. Morrison, P. J. Hergenrother and M. Movassaghi, Total Synthesis, Stereochemical Assignment, and Biological Activity of All Known (−)-Trigonoliimines, *J. Org. Chem.*, 2014, **79**, 473–486.
88 T. Teraoka, S. Hiroto and H. Shinokubo, Iridium-Catalyzed Direct Tetraborylation of Perylene Bisimides, *Org. Lett.*, 2011, **13**, 2532–2535.
89 C. L. Lyall, C. C. Shotton, M. Pérez-Salvia, G. Dan Pantoș and S. E. Lewis, Direct core functionalisation of naphthalenediimides by iridium catalysed C–H borylation, *Chem. Commun.*, 2014, **50**, 13837–13840.
90 Y. Jin, S. Hok, J. Bacsa and M. Dai, Convergent and Efficient Total Synthesis of (+)-Heilonine Enabled by C–H Functionalizations, *J. Am. Chem. Soc.*, 2024, **146**, 1825–1831.
91 V. Pace, P. Hoyos, L. Castoldi, P. Domínguez de María and A. R. Alcantara, 2-Methyltetrahydrofuran (2-MeTHF): A Biomass-Derived Solvent with Broad Application in Organic Chemistry, *ChemSusChem*, 2012, **5**, 369–1379.
92 L. Leist, C. Kerner, L. T. Ghoochany, S. Farsadpour, A. Fizia, J. P. Neu, F. Schön, Y. Sun, B. Oelkers, J. Lang, F. Menges, G. Niedner-Schatteburg, K. S. M. Salih and W. R. Thiel, Roll-over cyclometallation: A versatile tool to enhance the catalytic activity of transition metal complexes, *J. Organomet. Chem.*, 2018, **863**, 30–43.
93 B. Butschke and H. Schwarz, "Rollover" cyclometalation – early history, recent developments, mechanistic insights and application aspects, *Chem. Sci.*, 2012, **3**, 308–326.
94 K. M. Engle, T.-S. Mei, M. Wasa and J.-Q. Yu, Weak Coordination as a Powerful Means for Developing Broadly Useful C–H Functionalization Reactions, *Acc. Chem. Res.*, 2012, **45**, 788–802.
95 S. De Sarkar, W. Liu, S. I. Kozhushkov and L. Ackermann, Weakly Coordinating Directing Groups for Ruthenium(II)-Catalyzed C–H Activation, *Adv. Synth. Catal.*, 2014, **356**, 1461–1479.
96 E. M. Simmons and J. F. Hartwig, On the Interpretation of Deuterium Kinetic Isotope Effects in C–H Bond Functionalizations by Transition-Metal Complexes, *Angew. Chem., Int. Ed.*, 2012, **51**, 3066–3072.
97 D. G. Blackmond, Reaction Progress Kinetic Analysis: A Powerful Methodology for Mechanistic Studies of Complex Catalytic Reactions, *Angew. Chem., Int. Ed.*, 2005, **44**, 4302–4320.
98 C. D.-T. Nielsen and J. Burés, Visual kinetic analysis, *Chem. Sci.*, 2019, **10**, 348–353.
99 N. Le, N. L. Chuang, C. M. Oliver, A. V. Samoshin, J. T. Hemphill, K. C. Morris, S. N. Hyland, H. Guan, C. E. Webster and T. B. Clark, Hidden Role of Borane in Directed C–H Borylation: Rate Enhancement through Autocatalysis, *ACS Catal.*, 2023, **13**, 12877–12893.
100 I. F. Yu, J. L. Manske, A. Diéguez-Vázquez, A. Misale, A. E. Pashenko, P. K. Mykhailiuk, S. V. Ryabukhin, D. M. Volochnyuk and J. F. Hartwig, Catalytic undirected borylation of tertiary C–H bonds in bicyclo[1.1.1]pentanes and bicy-clo[2.1.1]hexanes, *Nat. Chem.*, 2023, **15**, 685–693.
101 S. Ghosh, T. Khandelia and B. K. Patel, Solvent-Switched Manganese(I)-Catalyzed Regiodivergent Distal vs Proximal C–H Alkylation of Imidazopyridine with Maleimide, *Org. Lett.*, 2021, **19**, 7370–7375.
102 C. Yu, J. Sanjosé-Orduna, F. W. Patureau and M. H. Pérez-Temprano, Emerging unconventional organic solvents for C–H bond and related functionalization reactions, *Chem. Soc. Rev.*, 2020, **49**, 1643–1652.
103 Y. Niu, C.-X. Yan, X.-X. Yang, P.-B. Bai, P.-P. Zhou and S.-D. Yang, Solvent-controlled regioselective arylation of indoles and mechanistic explorations, *Org. Chem. Front.*, 2022, **9**, 1023–1032.
104 H. F. Motiwala, A. M. Armaly, J. G. Cacioppo, T. C. Coombs, K. R. K. Koehn, V. M. Norwood IV and J. Aubé, HFIP in Organic Synthesis, *Chem. Rev.*, 2022, **122**, 12544–12747.
105 W. Jo, C. Thangsrikeattigun, C. Ryu, S. Han, C. Oh, M.-H. Baik and S. H. Cho, Regiodivergent Alkylation of Pyridines: Alkyllithium Clusters Direct Chemical Reactivity, *J. Am. Chem. Soc.*, 2025, **147**, 8597–8606.
106 (*a*) CCDC 2480983: Experimental Crystal Structure Determination, 2026, DOI: **10.5517/ccdc.csd.cc2p8nqc**; (*b*) CCDC 2480984: Experimental Crystal Structure Determination, 2026, DOI: **10.5517/ccdc.csd.cc2p8nrd**; (*c*) CCDC 2480985: Experimental Crystal Structure Determination, 2026, DOI: **10.5517/ccdc.csd.cc2p8nsf**; (*d*) CCDC 2480986: Experimental Crystal Structure Determination, 2026, DOI: **10.5517/ccdc.csd.cc2p8ntg**; (*e*) CCDC 2480987: Experimental Crystal Structure Determination, 2026, DOI: **10.5517/ccdc.csd.cc2p8nvh**.